

Three-dimensional Detonation Cell Structures in a Circular Tube

D.-R., Cho, S.-H., Won, Edward J.-R., Shin, and J.-Y., Choi
Pusan National University, Busan, South Korea, 609-735
Seoul National University, Seoul, South Korea, 151-741
aerochoi@pusan.ac.kr

Keywords:

Abstract

Three-dimensional structures of detonation wave propagating in circular tube were investigated. Inviscid fluid dynamics equations coupled with a conservation equation of reaction progress variable were analyzed by a MUSCL-type TVD scheme and four stage Runge-Kutta time integration. Variable- γ formulation was used to account for the variable properties between unburned and burned states and the chemical reaction was modeled by using a simplified one-step irreversible kinetics model. The computational code was parallelized based on domain decomposition technique using MPI-II message passing library. The computations were carried out using a home made Windows based PC cluster having 160 AMD AthlonXP and Athlon64 processor. The computational domain consisted of through a round-shaped tube with wall conditions. As an initial condition, analytical ZND solution was distributed over the computational domain with disturbances. The disturbances has circumferential large gradient. The unsteady computational results in three-dimension show the detailed mechanisms of multi-cell mode of detonation wave instabilities resulting diamond shape in smoked-foil record

Introduction

Detonations are supersonic flow phenomena that consist of shock-induced combustion wave propagating through a reactive mixture or pure exothermic compound and of a thin reaction zone immediately behind the shock. They have been studied from the application engineering point of view, such as for propulsion application (i.e., Scramjet, Pulse Detonation Engines (PDEs), Oblique Detonation Wave Engines (ODWEs) and Rotating Detonation Engines (RDEs) etc.).

The detailed structures and properties of detonation have been shown experimental and numerical as well as theoretical method [1-10]. Experimental studies have been carried out by many researchers, who provide useful fundamental and practical data [4-6]. However, the detail three-dimensional structure of detonations has remained unclear because of its fast propagation speed and of the difficulty of three-dimensional visualization by experimental measurement devices. Recent studies of three-dimensional detonation have been shown that in a rectangular tube, the types of structure of detonation can be produced, namely, rectangular, diagonal and

spin detonation mode, where as a single spin mode and multi-cell (or multi-headed) detonation mode appears in a round tube. The detonation wave structure is inherently three-dimensional, but the experimental observation of the three-dimensional structure is very limited. Thus along with experimental efforts, there have been a considerable number of numerical studies of detonation to understand the three-dimensional detonation structure. In general, the fidelity of a numerical simulation relies on sharp capturing of the hydrodynamics discontinuities and on well-resolved representations of the reaction zone. Unfortunately, due to the large numbers of temporal and spatial scales associate with three-dimensional flows, the resolution requirements for three-dimensional simulations can easily exhaust most currently available computational resource. As a result, numerical three-dimensional results are particularly scarce. In thus far, only some researchers have presented such results for three-dimensional detonation structure.

Penyazkov et al. have investigated the evolution of detonation structure along the round tube and characterized it as a function of initial pressure by experimental study [4-5]. The other hand, triple point is characterized it a function of pre-exponential factor k on the numerical study [7]. By following-up previous the 3D rectangular tube analysis result, the purpose of present study is to understand and characterize of the 3D detonation structure in circular tube [8].

Numerical Approach

Governing Equations

The Euler equation of compressible inviscid flow with the conservation equation of reaction progress variable can be summarized the following vector form in a three-dimensional coordinate.

$$\frac{\partial Q}{\partial t} + \frac{\partial E}{\partial x} + \frac{\partial F}{\partial y} + \frac{\partial G}{\partial z} = H \quad (1)$$

where the conserved variable vector U , the flux vectors, E, F and G as well as the source vector H are given, respectively, as

$$Q = \begin{bmatrix} \rho \\ \rho u \\ \rho v \\ \rho w \\ \rho e \\ \rho Z \end{bmatrix} \quad E = \begin{bmatrix} \rho u \\ \rho u^2 + p \\ \rho uv \\ \rho uw \\ (\rho e + p)u \\ \rho Zu \end{bmatrix} \quad F = \begin{bmatrix} \rho v \\ \rho uv \\ \rho v^2 + p \\ \rho vw \\ (\rho e + p)v \\ \rho Zv \end{bmatrix} \quad (2a)$$

$$G = \begin{bmatrix} \rho w \\ \rho uw \\ \rho vw \\ \rho w^2 + p \\ (\rho e + p)w \\ \rho Zw \end{bmatrix} \quad H = \begin{bmatrix} 0 \\ 0 \\ 0 \\ 0 \\ 0 \\ \rho \dot{w} \end{bmatrix} \quad (2b)$$

Here u , v , and w are the components of the fluid velocity in the x , y , and z direction, respectively, in the Cartesian coordinates system, ρ is the density, p is the pressure and e is total energy per unit mass. The pressure is defined as,

$$p = (\gamma - 1)\rho \left[e - \frac{1}{2}(u^2 + v^2 + w^2) + Zq \right] \quad (3)$$

Here, Z is reaction progress variable that simulates the product mass fraction and varies from 0 to 1. q is the heat addition by combustion. Since gas properties of the unburned mixture and the combustion product are quite different, the use of constant gas property is not good enough. Thus a variable property formulation is employed in this study by interpolating the specific heat ratio of unburned and burned sides. The specific heat ratio has more complex form as Eq. (4) to satisfy the conservation law and ideal gas assumption.

$$\gamma(Z) = \frac{\gamma_U(\gamma_B - 1)(1 - Z) + \gamma_B(\gamma_U - 1)Z}{(\gamma_B - 1)(1 - Z) + (\gamma_U - 1)Z} \quad (4)$$

As a combustion mechanism, one-step Arrhenius reaction model are used to simulate the various regimes of detonation phenomena without the complexity and large computing time for dealing with many reaction step and detailed properties of reaction species. Thus, the reaction rate in Eq. (1) that depends on mixture concentration is defined as follows.

$$\dot{w} = (1 - Z)k \exp(-E_a \rho / p) \quad (5)$$

Thermo-chemical Parameters and Computational Domain

Since the purpose of present study to understand the fundamental and characterize of the 3D detonation structure in circular tube, the computational cases was restricted to weakly unstable detonation. The thermo-chemical parameters were for the simulation was selected from Austine et al. [6]. The unburned and burned specific heat ratios are $\gamma_U = 1.602$ and $\gamma_B = 1.288$. Dimensionless heat addition is $q = 24.2$. Dimensionless activation energy by von Neumann peak temperature is $\theta = E_a / RT_{VN} = 5.2$, which exhibits weakly unstable detonation waves. The pre-exponential factor, k , has direct relation with grid resolution. Here, the k is selected in between 1,000 to 2,000.

The computational mesh is a cylindrical system with 326(axial direction) \times 41(radial direction) \times 164(circumferential direction), 326 \times 41 \times 82 and 164 \times 41 \times 82 grid points. The computational grid system is show in Fig. 1. The tube diameter is unity and the length of the uniform section is 2. The rear

part is composed of smoothly extended grid for a long distance to ensure the C-J condition at the exit boundary. The length of the computational domain was selected to maintain the stabilized regular detonation wave oscillation within the uniform section of the computational domain.

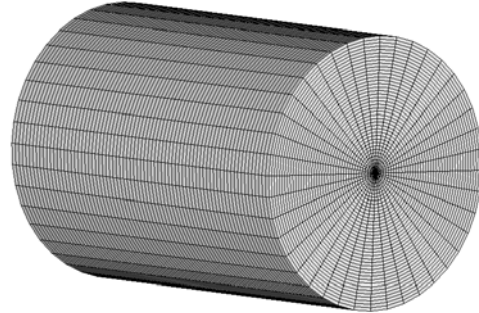


Fig.1 Computational grid system. A grid point for every four points in the axial and circular directions is plotted. The plotted axial length is one-half

Initial and Boundary Conditions, and Solution Algorithms

As initial condition of the simulation of detonation wave propagation, the results of the ZND structures calculation were used by setting the ZND solutions along the every grid line in longitudinal direction. For fast initial of the unstable motion, artificial perturbation should be introduced into the initial condition.

The incoming boundary condition was used with C-J detonation speed, that corresponds to the overdrive factor, $f = (U_\infty / U_{C-J})^2 = 1.0$. The wall is assumed be slip wall and adiabatic. The exit boundary condition was used base on the characteristic boundary condition using C-J condition as a far-field condition, as follows.

$$p_{exit} = p_{C-J} \quad (6a)$$

$$\rho_{exit} = \rho_1 + (p_{exit} - p_1) / c_{C-J}^2 \quad (6b)$$

$$u_{exit} = u_1 + (p_{exit} - p_1) / (\rho c)_{C-J} \quad (6c)$$

Here, transverse velocity component is simply extrapolated and the subscript 1 stands for the value in the first cell near the boundary.

The fluid dynamics equations are discretized by finite volume cell-vertex formulation. The numerical fluxes at cell interfaces are calculated by means of Roe's approximate Riemann solver with interpolated primitives variables by third-order accurate MUSCL-TVD scheme. The discretized equation was integrated in time by 4th order accurate Runge-Kutta scheme. Computational code was parallelized by MPI-II message-passing library by domain decomposition technique. The parallel computation was carried out with the home-built Windows PC cluster system.

Result and Discussion

Grid Refinement Study

Fig. 2 is the comparison of the numerical smoked-foil record from different grid solution at time for the same thermo-fluidic conditions. It is found that the detonation cell size is nearly same for all the grid resolutions although the sharpness of the cell pattern is different due to the different grid resolutions. The computation was carried out for $k=1,000$, that resulted two cell width for the unit tube diameter. Starting from the initial distribution, unstable of cell structure is developed. After some period of advancement, cell structure is stabilized to a regular pattern. In regular pattern zone, the detonation front continuously regenerates the same number of equal-size cells per tube perimeter, and cells width is $\lambda = \pi d/N$. Here, d is the tube diameter and N is the integer number, which equals to the order of detonation mode or the generated cell number. Fig. 2 is two-cell detonation mode, $N = 2$, and cell width is $\lambda = \pi/2$.

Two-Cell Detonation Mode

Fig.3 is shows the time-evolution of the detonation front wave structures at $k=1,000$. Here, “I” is number of iterations. The wave structure’ oscillations of two-cell mode are observed from this result. Here, a number of iterations of oscillation period are about 8,000. So the detonation wave structure at $I=108,000$ is same as $I=100,000$. In the fig. 3, the wave front structure is simulated well the front-end experimental soot imprint films in the fig. 6. Fig. 4 is shows the leading shock wave front and rear side structure in two cell detonation mode. In rear side figure, the arrows indicate the moving direction of transverse waves and the parts of green color are higher pressure zone. These parts can be considered as triple point on the wall. The smoked-foil record is trajectory (or history) of triple point moving on the wall. So from the fig. 4-(b), we can find that detonation wave structure has the four transverse waves moving along the circumference and two transverse waves moving along the radius direction, respectively. By the moving of four transverse waves, it means that the moving of four triple point, the two-cell mode’s smoked-foil record pattern is recorded on the wall. And by two transverse waves, these can be regarded as two triple-lines, and four transverse waves, the soot imprint films of two-cell mode are made on the front-end in the round tube. Specially, the characteristic wave front structures of two-cell mode are generated by two transverse waves in radius direction. We can find easily it from the comparison between the wave front structures of numerical simulation in the fig. 3 and the experimental soot imprint films in the fig. 6. Fig. 5 is numerical smoked-foil record with $326 \times 41 \times 164$ grid and $k=1,000$ by moving of the four transverse waves. The smoked-foil is shows that cell structure is stabilized to a regular pattern after some period of advancement. This numerical smoked-foil record is simulated very well the experimental result in the fig. 6. Here, the cell width is $\lambda = \pi/2$, $N=2$, in tube perimeter.

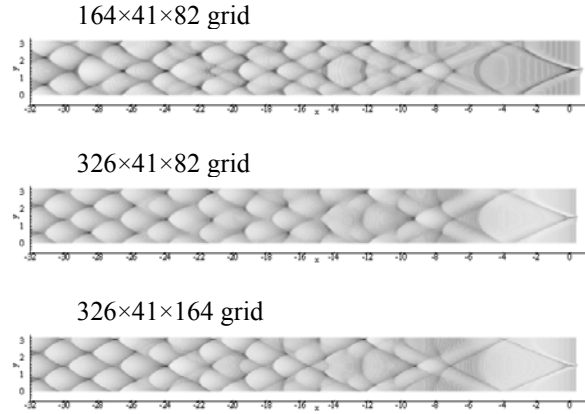


Fig. 2 Numerical smoked-foil records for three-different grid resolution, pre-exponential factor $k=1,000$.

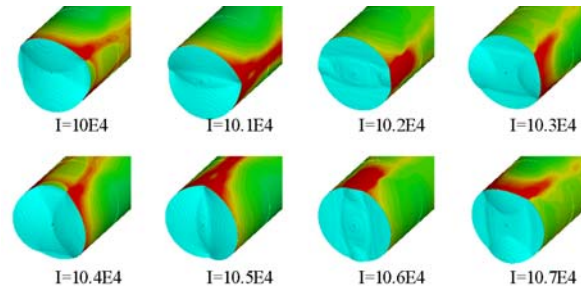


Fig. 3 Evolutions of detonation wave oscillation on regular zone in the two-cell detonation mode

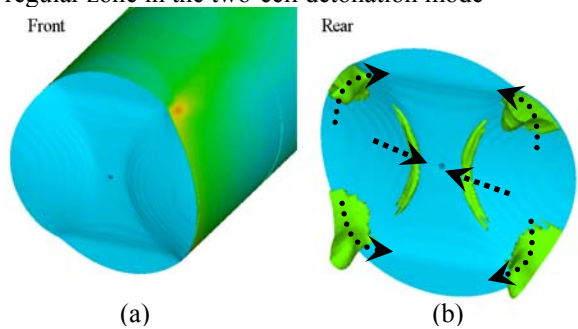


Fig. 4 The leading shock wave front (a) and rear side (b) structure in the two-cell detonation mode, respectively.

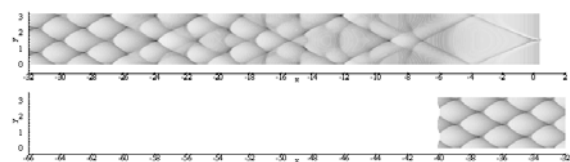


Fig. 5 Numerical smoked-foil records for two-cell detonation mode with $326 \times 41 \times 164$ grid, $k=1,000$.

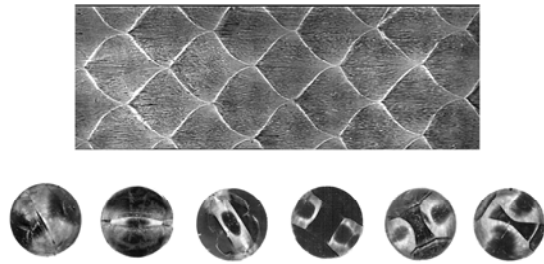


Fig. 6 Experimental soot imprint films for two-cell detonation mode in a round tube' wall and front-end, by O.G. Penyazkove⁵

Three-Cell Detonation Mode

Here, the pre-exponential value is increased to $k=1,500$. Fig. 7 is shows the time-evolution of the detonation front wave structures. The wave oscillations of the three-cell mode are observed from this result. It is shows that detonation wave structure has six transverse waves along the circumference and three transverse waves along the radius direction, respectively. The more detailed structures are observed in the fig 8. Fig. 8-(b) is shown very well the detonation wave structures that the six transverse waves move in the circumference direction and the three transverse waves move in radius direction, respectively. Fig. 9 is numerical smoked-foil record with $326 \times 41 \times 82$ grid at $k=1,500$ and fig. 10 is experimental smoked-foil record. The numerical smoked-foil is shows that cell structure is stabilized to a regular pattern after some period of advancement. In the regular pattern zone, the numerical smoked-foil record is simulated very well the experimental result in the fig. 10. In the figure from 7 to 10, we can find that the transverse waves, i.e. the six triple points and the three triple lines, are arranged repeatedly to the regular triangle shape and the windmill shape with the jointed three triple lines in the center of circle at the regeneration point of cell. At this point the triple points are reduced to three and the internal angle of triangle meets the each other at 60 degrees. So from the one triple point to the others, the differential of phase angle or an included angle of the triple lines in the windmill shape case is 120 degrees.

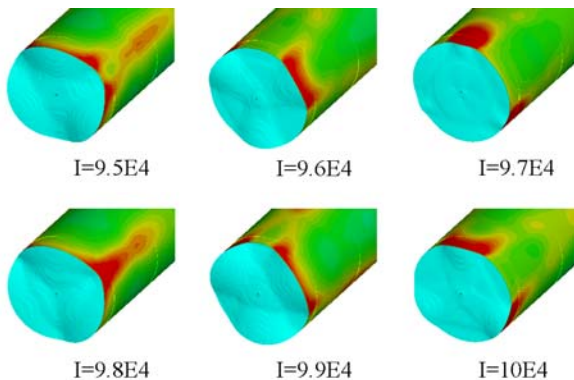


Fig. 7 Evolutions of detonation wave oscillation in the three-cell mode

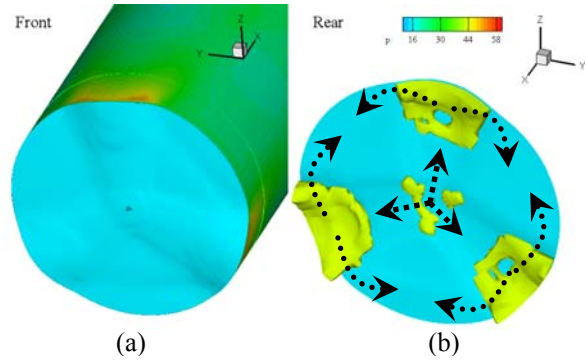


Fig. 8 The leading shock wave front (a) and rear side (b) structure in the three-cell mode, respectively.

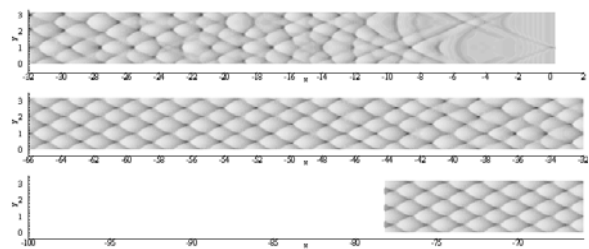


Fig. 9 Numerical smoked-foil records for three-cell mode with $326 \times 41 \times 82$ grid, $k=1,500$.

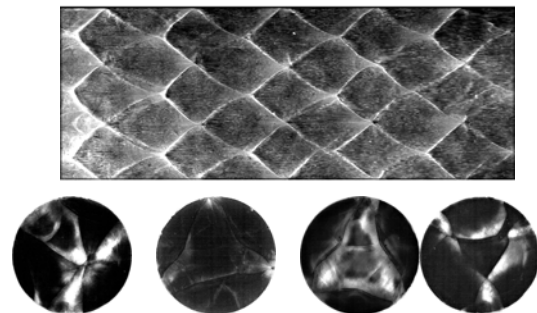


Fig. 10 Experimental soot imprint films for three-cell mode in a round tube' wall and front-end, by O.G. Penyazkove⁵

In the two-cell mode, the triple point is in position on the opposite side of the each other, i.e. the differential of phase angle is 180 degrees. And it is reduced to 90 degrees in the four cell mode. The cell width is $\lambda = \pi/3$, $N=3$, in tube perimeter. The cell width and length is about 2/3 time of two-cell mode.

Four-Cell Detonation Mode

In the fig. from 11 to 13, the number of moving transverse waves in the circumference and radius direction, the generated mechanism of smoked foil record and the oscillation of detonation wave structure by the moving of transverse waves can be understand easily in the four cell mode. Fig. 11 is shows the time-evolution of the detonation front wave structures at $k=2,000$. The wave oscillations of the four-cell mode are observed from this result. It shows that detonation wave structure has eight transverse waves along the

circumference and four transverse waves along the radial direction, respectively. We can find more easily it from the fig. 12. The wave structures are arranged repeatedly to the regular rectangular shape and the windmill shape of the jointed triple lines in the center of circle at the regeneration point of cell. At this time, an included angle of jointed triple lines is 90 degrees.

Fig. 13 is smoked-foil record with 326x41x82 grid and $k=2,000$. The smoked-foil is shows that cell structure is stabilized to a regular pattern after some period of advancement as the two- and three-cell mode. The cell number is increased but cell length and width are decreased same as three-cell mode. The cell width is $\lambda = \pi/4$, $N=4$, in tube perimeter. The cell width and length is about (or exactly) half of two-cell mode.

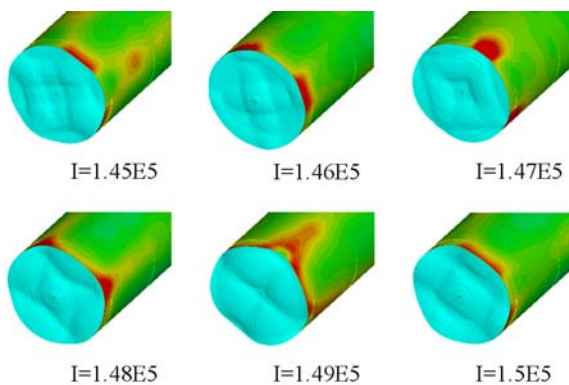


Fig. 11 Evolutions of detonation wave oscillation in the four-cell mode.

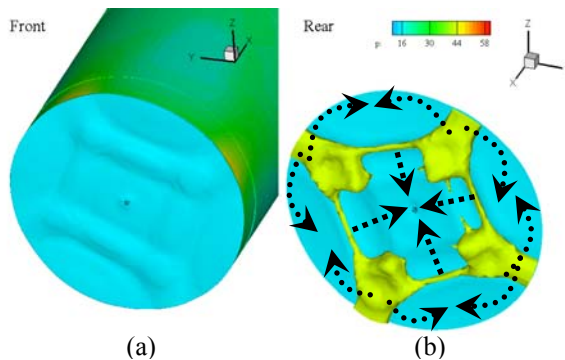


Fig. 12 The leading shock wave front (a) and rear side (b) structure in the four-cell mode, respectively.

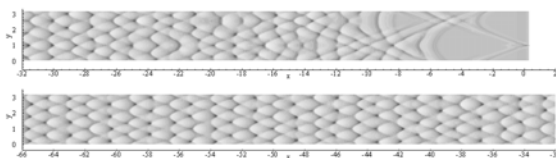


Fig. 13 Numerical smoked-foil records in the four-cell mode with 326x41x82 grid, $k=2,000$.

Conclusion

Unsteady three-dimensional simulations were performed in a circular tube and multi-cell detonation was simulated. The unsteady results in three-dimension showed the mechanisms of two, three and four cell mode of detonation wave. A two-, three- and four-cell detonation mode has four, six, eight transverse wave along circumference and two, three, four transverse wave along the radius, respectively. In the all detonation mode, we investigated that the detonation wave structures and smoked-foil records on the wall are made by the moving of transverse waves. And we can find that the detonation wave fronts are constructed the regular polygon shape and windmill shape with multi-vanes - a number of two, three and four vanes in the two-, three- and four cell mode, respectively - at the cell-regeneration point on the regular cell pattern zone. Also it came to conclusion that the multi-cell mode of detonation wave is characterized by pre-exponential factor k in a circular tube. It was confirmed that the cell number was increased but cell width and length were decreased with increased pre-exponential factor or the number of cell mode.

References

- 1) Fickett, W., and Davis, W.C.: Detonation Theory and Experiment, Dover Publications, New York, 2000
- 2) Tsuboi, N., Hayasi, A.K.: Numerical study on spinning detonations, Proceeding of the Combustion institute, vol.31, Issue2, 2007, pp.2389-2396.
- 3) Tsuboi, N., Eto, K., Hayashi, A.K.: Detailed structure of spinning detonation in a circular tube, Combustion and Flame vol.149 2007, pp.144-161.
- 4) Achasov, O.V., Penyazkov, O.G.: Dynamics study of detonation-wave cellular structure I. Statistical properties of detonation wave front, Shock Waves vol.11 2002, pp.297-308.
- 5) Penyazkov, O.G., Sevrouk, K.L.: On critical conditions of the flow within the cellular detonation structure, 21st ICDERS July. 2007.
- 6) Austin, J.M., Pintgen, F. and Shepherd, J.E.: Reaction Zones in Highly Unstable detonations, Proceedings of the Combustion Institute, Vol.30, No.2, 2005, pp. 1849-1858.
- 7) Choi, J.-Y., Ma, F. and Yang, V.: Numerical Simulation of Cellular Structure of Two-Dimensional Detonation Waves, AIAA Paper 2005-1174, 43rd AIAA ASM, Jan. 10-13, 2005, Reno, NV.
- 8) Tsuboi, N., Katoh, S. and Hayashi, A.K.: Three-Dimensional Numerical Simulation for Hydrogen/Air Detonation: Rectangular and diagonal Structures, Proceeding of the Combustion Institute, Vol. 29, 2002, pp. 2783-2788.
- 9) Deledicque, V. and Papalexandris, M.V.: Computational study of three-dimensional gaseous detonation structures, Combustion and Flame, Vol. 144, 2006, pp.821-837.
- 10) Gamezo, V.N., Desbordes, D., and Oran E.S.: Two-Dimensional Reactive flow Dynamics in Cellular Detonation Waves, Shock Waves, Vol. 9, 1999, pp. 11-17
- 11) Choi, J.-Y., Jeung, I.-S. and Yoon, Y.: Computational Fluid Dynamics Algorithms for Unsteady Shock-Induced Combustion, Part 1: Validation, AIAA Journal, Vol. 38m No. 7, July 2000, pp. 1179-1187.